

Fibre Bragg grating based spectral encoder/decoder for lightwave CDMA

A. Grunnet-Jepsen, A.E. Johnson, E.S. Maniloff, T.W. Mossberg, M.J. Munroe and J.N. Sweetser

An all-fibre technique for the coherent spectral encoding and decoding of optical pulses is proposed. The spectral coding of optical waveforms is achieved using pairs of oppositely chirped and suitably coded fibre gratings. The application potential to lightwave code-division-multiple-access (CDMA) communications is demonstrated.

Lightwave code-division-multiple-access (CDMA) provides multi-access communications in optical networks by introducing channel-specific code sequences that can be used for channel discrimination. Multiple users communicate over a common transport fibre by encoding optical bits with channel-specific codes. At the receivers, matched decoders distinguish the different channels using cross-correlation and thresholding operations. Of the numerous optical implementations of CDMA that have been proposed, variations have included encoding and decoding in the time and frequency domains and the use of coherent or incoherent signal processing [1–5]. One of the most widely investigated coherent signal-processing techniques [1–3] employs the spectral encoding of short pulses using the free-space 4F grating-pair configuration shown schematically in Fig. 1a. The 4F device consists essentially of two lenses, two uniform diffraction gratings and a spatial filter. The first lens is separated from the spatial filter by their focal lengths, F . The first grating-lens pair provides a mapping of the spectral content onto the position of the spatial filter. The second lens-grating pair recombines the filtered spectral components into a single beam. The transmission properties of the spatial filter determine the spectral coding function of the device. Code detection is effected with a similar 4F grating-pair device at the receiver end that produces autocorrelation spikes on the receipt of correctly coded signals. Despite the many promising features of this approach, application in the communications industry is hindered by the physical limitations of the 4F grating-pair devices. In practice, due to spectral resolution limits, 4F grating-pair devices work best with subpicosecond input pulses and produce autocorrelation signatures of similar duration. Consequently, CDMA based on 4F grating pair devices requires nonlinear means for detection and thresholding of correlation signals, and is subject to severe transmission impairments due to the ultra-wide bandwidth involved. It follows that CDMA based on 4F grating-pair devices has poor power sensitivity and limited transport range. Furthermore, the use of large free-space bulk-optics [1, 2] is not compatible with the robust compact packaging requirements of the telecommunications industry. It should be noted that interesting techniques have recently been suggested for implementing integrated optical devices offering functionality similar to that offered by the 4F

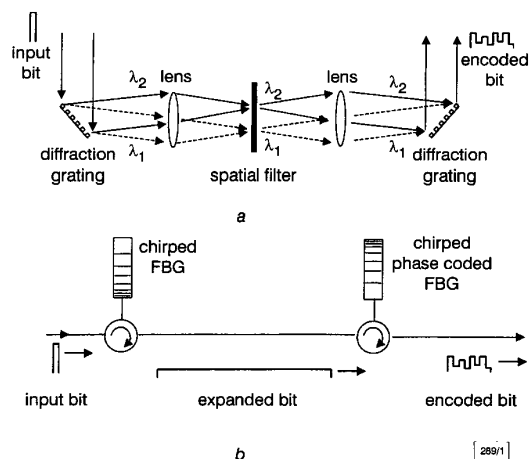


Fig. 1 Schematic diagram of spectral encoder using free-space diffraction gratings (DGs), and all-fibre construction based on pair of step-chirped fibre Bragg gratings (FBGs)

a DGs
b FBGs

grating-pair devices [3]. In this Letter, we present an all-fibre spectral-encoding approach based on temporal wavelength dispersion and recombination using fibre Bragg gratings (FBGs).

Fig. 1b shows a schematic diagram of the proposed all-fibre spectral phase encoder. The device consists of a pair of step-chirped FBGs arranged in series and is based on the concept of spectral dispersion in the time domain as opposed to the spatial Fourier domain. By step-chirped gratings, we mean gratings composed of spatially adjacent subgratings each of constant but constantly incremented spatial period. When an input bit is incident on the first chirped grating, the wavelengths are dispersed in time and the reflected pulse is temporally expanded. When this expanded bit is reflected from a second FBG having an opposite dispersion slope, the wavelength components are resynchronised and the original pulse is reconstituted. However, if the second grating contains phase-shifts along its length, these phase-shifts are transferred to the reflected signal and the output pulse represents a spectral-phase-encoded bit. Similarly, a spectral amplitude code can be impressed by varying the reflectivity of wavelength-selective grating subsections.

To ensure that each subgrating controls the backward diffraction of an isolated spectral band, the overall grating length should satisfy

$$L = \frac{N^2 \lambda_0^2}{2n \Delta \lambda} \quad (1)$$

where N is the number of subgratings, n is the effective refractive index, λ_0 is the carrier wavelength in air, and $\Delta \lambda$ is the optical bandwidth of the input bit. The contiguous subgratings have Bragg wavelengths that change by

$$\delta \lambda \approx \frac{\Delta \lambda}{N} \quad (2)$$

In the present demonstration, each grating consisted of $N = 8$ subgratings of length 2.4mm, arrayed contiguously for a total fibre grating length of 19.2mm. All subgratings are created in a single exposure through a patterned phase-mask. The subgratings in the first FBG have Bragg wavelengths that increase in 0.5nm steps from 1540.5nm (input signals see the 1540.5nm grating first). The subgratings of the second FBG are arranged in the reverse order and possess spatial phase shifts introduced during the grating fabrication. Each subgrating has a reflectivity of 60%. Fig. 2a shows an autocorrelation of an incident ~ 1 ps pulse and an expanded bit measured after reflection from the first FBG. The expanded bit was measured using a fast photodiode (12ps impulse response) and a 50GHz sampling oscilloscope. The temporal width corresponds well with the expected 192ps ($\tau_{mc} = 2nL/c$). Fig. 2b shows the measured temporal waveform after reflection from the second chirped and phase-coded FBG (shown together with the input pulse).

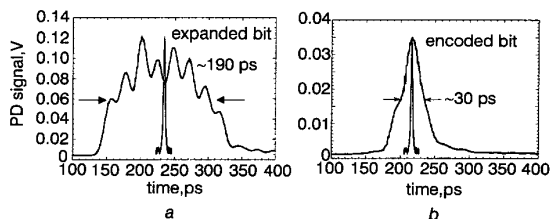


Fig. 2 Example of measured waveforms after first and second circulator of all-fibre spectral encoder shown together with ~ 1 ps input bit

a Expanded bit of width ~ 190 ps
b Encoded bit of width ~ 30 ps

Fig. 3a shows schematically the construction of a lightwave code-division multiaccess communication system using the proposed spectral encoders where each encoder has a complementary matched decoder. In the present demonstration, the encoder under investigation contains gratings G1 and G2. The matched receiver contains gratings G3 and G4, which are in essence identical to those of the encoder but connected in reverse. In other words, grating pair G1 and G2 are connected to the circulator with fibre ends that are the opposite of those of G3 and G4 in order to perform the time-reversed function of G1 and G2. After transmission of the encoded bit to the correctly matched decoder, the spectral

phase is essentially removed from the encoded waveform: the first grating in the decoder (G3) temporally disperses the spectral components and the second grating (G4) recombines the components and removes the phase code resulting in a short-duration decoded pulse.

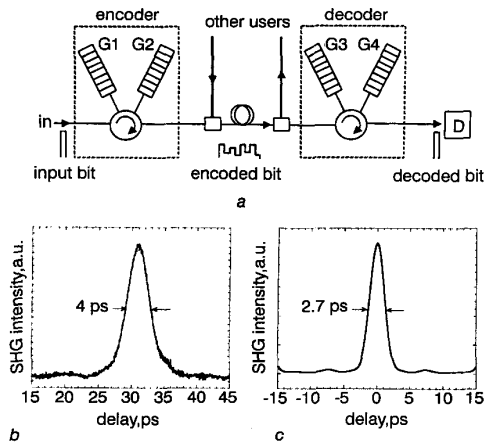


Fig. 3 Schematic diagram of optical-CDMA network based on all-fibre temporal-spectral encoders and decoders, and measured and predicted results for correctly decoded bits

- a Optical-CDMA network based on all-fibre temporal-spectral encoders and decoders
- b Measured intensity auto-correlation
- c Predicted intensity auto-correlation

The measured intensity autocorrelation of the decoded waveform in our demonstration is shown in Fig. 3b and the theoretical minimum-duration decoded waveform is shown in Fig. 3c. The minimum duration is determined by the ~ 4 nm bandwidth gratings used here and the ~ 1 ps input pulses. The discrepancy between the autocorrelation widths is believed to be due to a slight detuning between the spectra of the encoder and decoder gratings. As in all optical CDMA systems, the various channels in a multichannel system using spectral encoding are assigned different spectral codes such that the interference at the detector between correctly decoded signals and incorrectly decoded signals from other channels is minimal.

In summary, we have demonstrated an all-fibre method for the coherent spectral coding and decoding of pulses for use in code-division multiaccess communication systems. The fibre encoder and decoder functions are each equivalent to a 4F grating-pair spectral encoder. The use of fibre Bragg gratings for spectral phase coding provides several advantages over conventional free-space methods, most importantly compact system designs and longer processing times which permit the direct detection of decoded waveforms. The reconfigurability of codes may be incorporated by placing, for example, an electro-optic phase modulator between the encoding gratings which can shift the relative phases between the temporally dispersed spectral components in a controlled manner, or by physically controlling spatial phase shifts between subgratings. Finally, it should be noted that the functionality of the fibre grating-pair can also be achieved in a single grating by superimposing multiple gratings with predetermined grating spacing, amplitude and phase.

© IEE 1999
 Electronics Letters Online No. 19990722
 DOI: 10.1049/el:19990722

29 March 1999

A. Grunnet-Jepsen, A.E. Johnson, E.S. Maniloff, T.W. Mossberg, M.J. Munroe and J.N. Sweetser (Templex Technology, 400 E. 2nd Ave., Suite 101, Eugene, OR 97401, USA)

E-mail: templex@templex.com

References

- 1 SALEHI, J.A., WEINER, A., and HERITAGE, J.: 'Coherent ultrashort light pulse CDMA communication systems', *J. Lightwave Technol.*, 1990, LT-8, pp. 478-491

- 2 SARDESAL, H.P., CHANG, C.-C., and WEINER, A.M.: 'A femtosecond code-division multiple access communication system test bed', *J. Lightwave Technol.*, 1998, LT-16, pp. 1953-1964
- 3 KUROKAWA, T., TSUDA, H., OKAMOTO, K., NAGANUMA, K., TAKENOUCHI, H., INOUE, Y., and ISHII, M.: 'Time-space conversion optical signal processing using arrayed-waveguide grating', *Electron. Lett.*, 1997, 33, pp. 1890-1891
- 4 BABBITT, W.R., and MOSSBERG, T.W.: 'Optical waveform processing and routing with structured surface gratings', *Opt. Commun.*, 1998, 148, pp. 23-26
- 5 MARHIC, M.E.: 'Coherent optical CDMA networks', *J. Lightwave Technol.*, 1993, LT-11, pp. 854-864

Highly scalable OTDM router using computer controlled time slot tuner with picosecond resolution

R.J. Runser, K.-L. Deng, P. Toliver, I. Glesk and P.R. Prucnal

An OTDM router architecture using a highly scalable time slot tuner is discussed. Results for a 100Gbit/s, 16-channel router are presented. A maximum hardware time slot access latency of 3.2ns can be achieved with this architecture, enabling ultrafast optical packet routing.

Although lightwave technology is meeting the demand for point-to-point and long-haul transport of digital information, routing packets at the nodes of the network has typically been carried out using electronically switched backplane routers. The growing capacity on the Internet is placing an ever greater demand on electronic routing technologies. While wavelength division multiplexing (WDM) can support large aggregate traffic bandwidths, it is difficult to perform routing functions which may involve challenging techniques such as dense wavelength conversion. Additionally, present WDM laser and filter tuning techniques rely on slow technologies which increase the channel access latency and reduce the effective network bandwidth.

Recent advances in optical time division multiplexing (OTDM) have proven the capability of this technology in handling the switching and routing needs for future networks [1-3]. Channel access in OTDM networks is achieved by using time slot tuners and all-optical demultiplexers. Timing precision of < 1 ps is required to tune, multiplex, and demultiplex individual channels within the OTDM frame.

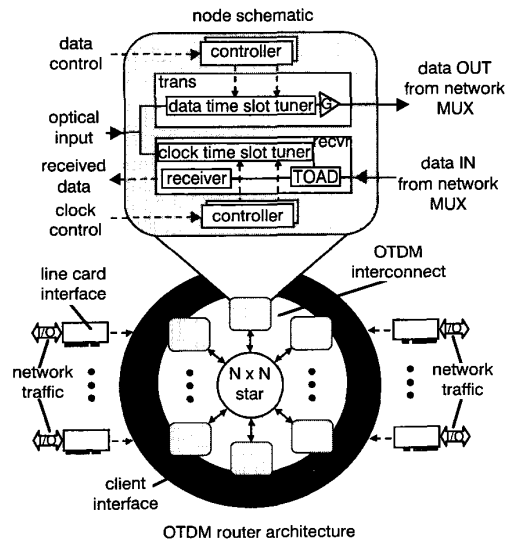


Fig. 1 OTDM node and router architecture

The router architecture we are constructing is based on an OTDM interconnect shown in Fig. 1. Like a standard electronic